

An SBFEM element for thin-walled beams

*J.D. Jung¹, W. Becker¹

¹Fachgebiet Strukturmechanik, Technische Universität Darmstadt, Germany.

*Corresponding author: jung@fsm.tu-darmstadt.de

Abstract

The scaled boundary finite element method (SBFEM) is a semi-analytical method in which only the boundary is discretized. The results on the boundary are scaled into the domain with respect to a scaling center which must be “visible” from the whole boundary. For beam-like problems the scaling center can be selected at infinity and only the cross-section is discretized.

A new element for thin-walled beams has been developed on the basis of the Reissner-Mindlin plate theory. The beam sections are considered to be multilayered laminate plates with arbitrary layup. The cross-section is discretized with beam elements of Timoshenko type. This leads to a system of differential equations of a gyroscopic type, for which the solution is known.

The element has been tested and compared with a finite element model and it gives good results.

Keywords: SBFEM, thin-walled beams, semi-analytical, Reissner-Mindlin theory

Introduction

Beams and beam-like structures are widely used in mechanical and civil engineering. Due to lightweight reasons these beams are often made of thin-walled sections. And recently new materials like fiber-reinforced plastics and other composites are used which are usually made of layers of differently oriented plies. With the number and the orientation of the plies and the order and the thickness of each ply there are many parameters, which can be adjusted during an optimization. Thus an effective and reliable computational method is needed.

The scaled boundary finite element method (SBFEM) is such a method. It is a semi-analytical method for which only a discretization of the boundary is needed and an analytical solution is used within the body. It doesn't need a singular fundamental solution like the boundary element method (BEM) or a discretization of the whole body like the FEM. So it has the benefits of both the FEM and the BEM without adopting the detriments.

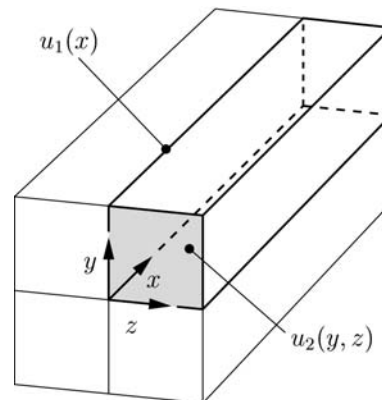


Figure 1: SBFEM for a beam

Let us start with a beam of arbitrary cross-section. This means that the cross-section does not need to be thin-walled. Then the SBFEM uses a separation approach to solve the differential equations for the displacements u in the framework of linear elasticity. The function u_1 scales the displacements of the boundary into the body. Or like in this work it scales the displacements of the cross-section along the beam. The boundary or the cross-section, respectively, is described by the function u_2 for which a finite element approach is used.

$$u(x, y, z) = u_1(x) \cdot u_2(y, z) \quad (1)$$

The coordinates y and z are on the cross-section (or the boundary) and x is directed along the beam axis (or into the body) which is depicted for a beam in figure 1.

Inserting this ansatz and the virtual work principle gives a differential equation of Euler-type (scaling center within the body) or of gyroscopic type (beam-like problem). For both differential equations the solution is known.

This method is a discrete Kantorovic method, which has been previously used also by other working groups, which is summarized below.

For an arbitrary 3-dimensional case Dasgupta (1982) published the first work about SBFEM and Wolf and Song (1996) developed this method further. First it was used to calculate the dynamic stiffness of an unbounded domain but body loads, incompressible material and bounded domains can be included in this method. Originally this method was called “consistent infinitesimal finite-element cell method” but using a different way to derive the equations the name “scaled boundary finite element method” (SBFEM) has been introduced (Wolf 2002).

Due to the analytical part of the solution the SBFEM can be used to calculate stress singularities at cracks which is done in (Wolf 2002) and in (Mayland and Becker 2010).

In Dieringer et al. (2011) thin plates are described by using 1D elements for the boundary. Here Kirchhoff’s kinematics is used to reduce the dimension by one.

For the case of slender cylindrical bodies like beams several groups developed similar or identical methods. The method developed at the University of Milan is equal to the SBFEM. In (Giavotto et al. 1983) the method is derived by introducing warping functions of the cross-section. These functions are only dependent on x . In (Morandini et al. 2010) the separation ansatz and a virtual work formulation are used. In contrast to this work, also 2D elements for the discretization of the cross-section are used. The aim is to calculate stiffnesses for the beam which are used in multi-body simulations.

Under the name “semi analytical finite elements” (Dong et al. 2001, Kosmatka et al. 2001, Lin et al. 2001) a method equal to the SBFEM is used to find de-Saint-Venant solutions. In (Alpdogan et al. 2010) this method is employed to examine end effects and transitional effects in prismatic beams. For the discretization 2D elements are used. In (Taweel et al. 2000) this method is extended for the calculation of wave reflections on free ends of cylinders. And in (Gavric 1994) the same is done for thin-walled beams using Kirchhoff-theory. One simplification is, that within an element the membrane and bending components do not interact.

Argyris and Kačianauskas (1996) use the same approach under the name SFE (Semi-analytical Finite Elements). Instead of the Dirichlet-Functional (virtual work principle) they employ the Hellinger-Reissner-Functional. 1D elements are used for the discretization of the cross-section of thin-walled beams. But only shear stresses and normal stresses in the direction of the beam axis are considered. Based on this theory they develop “semi-analytical based finite elements”.

Schardt (1989) developed a “generalized beam theory” for thin-walled beams. 1D elements are used for the discretization of the cross-section. But the Kirchhoff-theory is taken as framework and for sake of simplicity some stresses are neglected. Silvestre and Camotim (2002) extend this method for orthotropic materials where again some stresses are neglected.

In (Altenbach et al. 1994a) and (Altenbach et al. 1994b) a generalized Vlasov theory is developed. 1D elements and Kirchhoff’s plate theory are used. Neglecting stresses gives the theory of Schardt or Vlasov.

Artel and Becker (2006) use the SBFEM to calculate free-edge effects in laminates. 2D elements are employed to describe the boundary.

Theory

The theory is first presented for one element. The assembly of several elements is described later.

New coordinates (ξ , η and ζ) are introduced for each element. ξ is along the beam axis (x -axis) and η and ζ are in the cross-section (y,z plane). ξ and η are scaled so that they reach from 0 to 1.

Kinematics

The kinematics of a Reissner-Mindlin plate is presumed (Yang et al. 1966). One reason is that the Reissner-Mindlin theory is of higher order than the Kirchhoff-theory and includes transversal shear. Another reason is that a finite-element with Reissner-Mindlin theory has less unknown functions than an element based on Kirchhoff’s kinematic. The element with Kirchhoff’s kinematic has 8 degrees of freedom (dof) but gives an equation of 4th order. After linearization it has $8*4=32$ unknown functions. The Reissner-Mindlin element (as used here) has 11 dof, but the equation is only of 2nd order. Thus it has $11*2=22$ unknown functions.

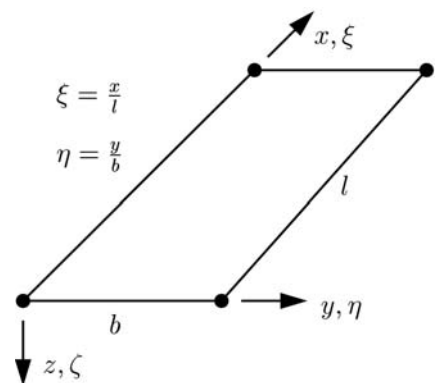


Figure 2: SBFEM Element

The key idea is that the displacements are traced back to the displacements and rotations of the middle plane (index 0)

$$\begin{aligned} u(\zeta, \eta, \zeta) &= u^0(\zeta, \eta) + \zeta \cdot \psi_\zeta(\zeta, \eta) \\ v(\zeta, \eta, \zeta) &= v^0(\zeta, \eta) + \zeta \cdot \psi_\eta(\zeta, \eta) \\ w(\zeta, \eta, \zeta) &= w^0(\zeta, \eta) \end{aligned} \quad (2)$$

where ζ and η denote the in-plane coordinates and ζ the coordinate in the thickness direction of the plate. The in-plane strains are given by

$$(\varepsilon_\xi, \varepsilon_\eta, \gamma_{\xi\eta}) = (\varepsilon_\xi^0, \varepsilon_\eta^0, \gamma_{\xi\eta}^0) + z \cdot (\kappa_\xi, \kappa_\eta, \kappa_{\xi\eta}) \quad (3)$$

and the out-of-plane strains are

$$\gamma_{\eta\zeta} = \gamma_{\eta\zeta}^0 = w_{,\eta}^0 + \psi_\eta \quad \gamma_{\xi\zeta} = \gamma_{\xi\zeta}^0 = w_{,\xi}^0 + \psi_\xi \quad \varepsilon_\zeta = 0 \quad (4)$$

where

$$\varepsilon_\xi^0 = u_{,\xi}^0 \quad \varepsilon_\eta^0 = v_{,\eta}^0 \quad \gamma_{\xi\eta}^0 = u_{,\eta}^0 + v_{,\xi}^0 \quad \kappa_\xi = \psi_{\xi,\zeta} \quad \kappa_\eta = \psi_{\eta,\zeta} \quad \kappa_{\xi\eta} = \psi_{\xi,\eta} + \psi_{\eta,\xi} \quad (5)$$

In total this can be written as a matrix equation

$$\boldsymbol{\varepsilon} = \mathbf{L} \cdot \mathbf{u} \quad (6)$$

where $\boldsymbol{\varepsilon}$ comprises all strain components, \mathbf{u} comprises the midplane displacements and rotations and \mathbf{L} denotes a respective differential operator.

Constitutive relations

The constitutive relations are the ones proposed by Yang et al. (1966) where the classical laminate theory (CLT) is extended and the shear strains $\gamma_{\eta\zeta}$ and $\gamma_{\xi\zeta}$ and the shear stresses $\tau_{\eta\zeta}$ and $\tau_{\xi\zeta}$ are included.

The stresses are integrated over the thickness h of the plate

$$\begin{aligned} (N_\xi, N_\eta, N_{\xi\eta}) &= \int (\sigma_\xi, \sigma_\eta, \tau_{\xi\eta}) d\zeta, \quad (M_\xi, M_\eta, M_{\xi\eta}) = \int (\sigma_\xi, \sigma_\eta, \tau_{\xi\eta}) \zeta d\zeta, \\ (Q_\xi, Q_\eta) &= \int (\tau_{\xi\zeta}, \tau_{\eta\zeta}) d\zeta \end{aligned} \quad (7)$$

which gives the normal and shear forces N_ξ , N_η and $N_{\xi\eta}$, the bending and drilling moments M_ξ , M_η and $M_{\xi\eta}$ and the transversal forces Q_ξ and Q_η .

These cross-sectional forces are related to the strains and curvatures by a corresponding laminate stiffness Matrix \mathbf{C}

$$\begin{pmatrix} N_\xi \\ N_\eta \\ Q_\xi \\ Q_\eta \\ N_{\xi\eta} \\ M_\xi \\ M_\eta \\ M_{\xi\eta} \end{pmatrix} = \begin{pmatrix} A_{11} & A_{12} & 0 & 0 & A_{16} & B_{11} & B_{12} & B_{16} \\ A_{12} & A_{22} & 0 & 0 & A_{26} & B_{12} & B_{22} & B_{26} \\ 0 & 0 & A_{44} & A_{45} & 0 & 0 & 0 & 0 \\ 0 & 0 & A_{45} & A_{55} & 0 & 0 & 0 & 0 \\ A_{16} & A_{26} & 0 & 0 & A_{16} & B_{16} & B_{26} & B_{66} \\ B_{11} & B_{12} & 0 & 0 & B_{16} & D_{11} & D_{12} & D_{16} \\ B_{12} & B_{22} & 0 & 0 & B_{26} & D_{12} & D_{22} & D_{26} \\ B_{16} & B_{26} & 0 & 0 & B_{66} & D_{16} & D_{26} & D_{66} \end{pmatrix} \begin{pmatrix} \varepsilon_\xi^0 \\ \varepsilon_\eta^0 \\ \gamma_{\xi\eta}^0 \\ \gamma_{\xi\zeta}^0 \\ \gamma_{\eta\zeta}^0 \\ \kappa_\xi \\ \kappa_\eta \\ \kappa_{\xi\eta} \end{pmatrix} \quad (8)$$

where the stiffness coefficients for a laminate plate with n layers are defined by

$$(A_{ij}, B_{ij}, D_{ij}) = \sum \int \overline{Q_{ij}^m} (1, \zeta, \zeta^2) d\zeta \quad (9)$$

Herein the quantities $\overline{Q_{ij}^m}$ denote the reduced stiffnesses of a single orthotropic layer. See (Yang et al. 1966) for further information.

Scaled boundary finite element approach

In the present SBFEM approach the degrees of freedom are the displacements u , v and w and the angles of rotations Ψ_ξ and Ψ_η . A linear shape function for u , v , Ψ_ξ and Ψ_η is chosen. For w a quadratic function is used to avoid shear locking of the plate. This corresponds to the ‘‘consistent interpolation Timoshenko beam element’’ described in (Reddy 1997). It gives an element which has 11 degrees of freedom, as indicated in figure 3.

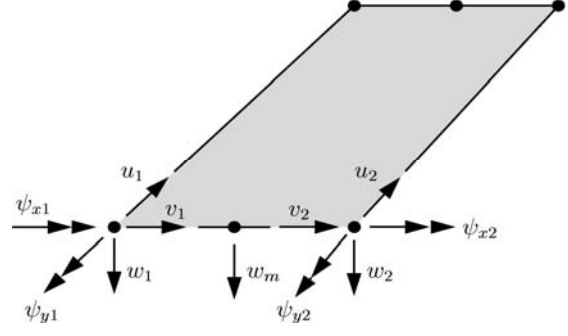


Figure 3: Degrees of freedom of an element

The SBFEM approach can briefly be written as

$$\mathbf{u}(\zeta, \eta) = \mathbf{N}(\eta) \cdot \mathbf{u}_e(\zeta) \quad (10)$$

where \mathbf{u} are the displacements and rotations, \mathbf{N} the matrix containing the shape functions and \mathbf{u}_e the vector with the degrees of freedom of the element.

Virtual work principle

The virtual work principle is given by

$$\delta \Pi_i = \int \delta \boldsymbol{\varepsilon} \cdot \boldsymbol{\sigma} dV = \int \delta \mathbf{u} \cdot \mathbf{p} dV + \int \delta \mathbf{u} \cdot \mathbf{t} dA = -\delta \Pi_a \quad (11)$$

where δ indicates virtual displacements and strains. \mathbf{p} denotes the volume forces and \mathbf{t} the forces at the boundary. Using the kinematics and the scaled boundary finite element approach for the displacements gives

$$\boldsymbol{\varepsilon}(\zeta, \eta) = \mathbf{L}\mathbf{u} = \mathbf{L}\mathbf{N}(\eta)\mathbf{u}_e(\zeta) = \mathbf{B}\mathbf{u}_e = \left(\mathbf{B}_2 + \mathbf{B}_1 \frac{\partial}{\partial \zeta} \right) \mathbf{u}_e \quad (12)$$

The matrix \mathbf{B} can be divided into two parts. The first one contains the derivatives with respect to η and the second one the derivatives with respect to ζ . Inserting these representations into the virtual work principle and using the constitutive equation gives

$$\begin{aligned} \delta \Pi_i &= \int \delta \mathbf{u}_e^T \left(-\frac{1}{l} \mathbf{E}_0 \mathbf{u}_{e,\zeta\zeta} + (\mathbf{E}_1 - \mathbf{E}_1^T) \mathbf{u}_{e,\zeta} + l \mathbf{E}_2 \mathbf{u}_e \right) dx + \delta \mathbf{u}_e^T \left(\frac{1}{l} \mathbf{E}_0 \mathbf{u}_{e,\zeta} + \mathbf{E}_1^T \mathbf{u}_e \right) \Big|_{x=0}^{x=l} = \dots \\ &\dots = \int \delta \mathbf{u}_e^T l \left(\bar{\mathbf{p}} + \mathbf{f}^s(x, b) - \mathbf{f}^s(x, 0) \right) dx + \left(\delta \mathbf{u}_e^T \mathbf{f}(\zeta) \right) \Big|_{x=0}^{x=l} = -\delta \Pi_a \end{aligned} \quad (13)$$

where the matrices \mathbf{E}_i are

$$\mathbf{E}_0 = \int \mathbf{B}_1^T \mathbf{C} \mathbf{B}_1 b d\eta, \quad \mathbf{E}_1 = \int \mathbf{B}_2^T \mathbf{C} \mathbf{B}_1 b d\eta, \quad \mathbf{E}_2 = \int \mathbf{B}_2^T \mathbf{C} \mathbf{B}_2 b d\eta \quad (14)$$

and the forces at the boundary and the volume forces are given by

$$\mathbf{f}^s(\zeta, \eta) = \mathbf{N}^T(\eta) \begin{pmatrix} N_{\zeta\eta}(\zeta, \eta) \\ N_\eta(\zeta, \eta) \\ Q_\eta(\zeta, \eta) \\ M_{\zeta\eta}(\zeta, \eta) \\ M_\eta(\zeta, \eta) \end{pmatrix}, \quad \mathbf{f}(\zeta) = \int \mathbf{N}^T(\eta) \begin{pmatrix} N_\zeta(\zeta, \eta) \\ N_{\zeta\eta}(\zeta, \eta) \\ Q_\zeta(\zeta, \eta) \\ M_\zeta(\zeta, \eta) \\ M_{\zeta\eta}(\zeta, \eta) \end{pmatrix} b d\eta, \quad \bar{\mathbf{p}} = \int \mathbf{N}^T(\eta) \mathbf{p}(\zeta, \eta) b d\eta \quad (15)$$

Here \mathbf{f}^s are the forces at the side-faces of the element ($\eta=0$ and $\eta=1$). \mathbf{f} are the forces at the ends of the element ($\zeta=0$ and $\zeta=1$) and $\bar{\mathbf{p}}$ contains the volume forces. The load vector \mathbf{p} (Yang et al. 1966) is defined by

$$\mathbf{p} = (p_\zeta \quad p_\eta \quad p_\zeta \quad P_\zeta \quad P_\eta)^T = \left(\int f_\zeta d\zeta \quad \int f_\eta d\zeta \quad \int f_\zeta d\zeta \quad \int f_\zeta \zeta d\zeta \quad \int f_\eta \zeta d\zeta \right)^T \quad (16)$$

The virtual displacement $\delta \mathbf{u}_e$ is arbitrary and thus the equation

$$-\frac{1}{l} \mathbf{E}_0 \mathbf{u}_{e,\xi\xi} + (\mathbf{E}_1 - \mathbf{E}_1^T) \mathbf{u}_{e,\xi} + l \mathbf{E}_2 \mathbf{u}_e = l (\bar{\mathbf{p}} + \mathbf{f}^s(x,b) - \mathbf{f}^s(x,0)) \quad (17)$$

and the boundary condition

$$\frac{1}{l} \mathbf{E}_0 \mathbf{u}_{e,\xi} + \mathbf{E}_1^T \mathbf{u}_e = \mathbf{f}(\xi) \quad (18)$$

have to be fulfilled.

In the further work only the homogeneous differential equation (17) is considered. The volume forces $\bar{\mathbf{p}}$ and the forces at the side-faces (\mathbf{f}^s) are supposed to vanish.

Assembling several elements

Above the equations for one element are given. For each element j the matrices \mathbf{E}_{ij} are calculated in the local coordinate system. After that these elements have to be assembled.

Using elements which are oriented differently gives a problem. There are 5 degrees of freedom in the element, but 6 degrees of freedom are needed when joining elements with different normal directions. In figure 4 this problem is depicted. From the point of view of plate 2 the rotation Ψ_ζ about the plate normal is missing.

For nodes in edges this additional degree of freedom $\Psi_{\zeta i}$ is introduced. The vector \mathbf{u}_e for elements containing this node becomes

$$\mathbf{u}_e = (u_1 \quad v_1 \quad w_1 \quad \psi_{\xi 1} \quad \psi_{\eta 1} \quad \psi_{\zeta 1} \quad u_2 \quad v_2 \quad w_2 \quad \psi_{\xi 2} \quad \psi_{\eta 2} \quad \psi_{\zeta 2} \quad w_m)^T \quad (19)$$

The matrices \mathbf{E}_{ij} for these elements get additional columns and rows with zero entries. Nodes in the middle of an element and nodes where the elements are in one plane don't need this additional degree of freedom. So for further calculations they are left in local coordinates.

The degrees of freedom for these edge-nodes are transformed into a global coordinate system which is done by a rotation about the ξ -axis (using the rotation matrix \mathbf{T}).

These transformed matrices \mathbf{E}_{ij}^g can be given by

$$\mathbf{E}_{ij}^g = \mathbf{T} \mathbf{E}_{ij}^l \mathbf{T}^T \quad (20)$$

and they are assembled by adding up the matrices for each element. This gives an SBFEM equation which has the same form like the one for a single element. But the unknowns are \mathbf{u} , which contains the degrees of freedom of all nodes and the matrices \mathbf{E}_i^g , which are the assembly of the \mathbf{E}_{ij}^g .

The resulting SBFEM equation is of a gyroscopic type (see Tisseur and Meerbergen 2001). \mathbf{E}_0 is symmetric and positive definite and \mathbf{E}_2 is positive semidefinite with 4 zero-eigenvalues and $\mathbf{E}_1 - \mathbf{E}_1^T$ is antisymmetric. Thus the eigenvalues are symmetric to the real and the imaginary axis.

As explained in (Morandini et al. 2010) this problem has 12 zero-eigenvalues and only 4 corresponding eigenvectors. These eigenvectors describe the rigid-body displacements and the rotation around the ξ -axis. There are two Jordan-Blocks of size 2 which also describe the torsion and the strain of a de-Saint-Venant problem. The two other blocks are of size 4 and describe the rotation about the η - and ζ -axis and the bending of a de-Saint-Venant beam due to forces and moments.

The solutions with non-zero eigenvalues describe end-effects which decrease exponentially.

Solution process

The SBFEM equation (17) is solved via a matrix exponential as it has been proposed by Song (2004). So first of all it has to be transformed into a linear matrix differential equation. For this purpose new variables $\tilde{\mathbf{u}}$ are introduced which are defined by

$$\tilde{\mathbf{u}} = l \cdot \mathbf{u}_{,\xi} \quad (21)$$

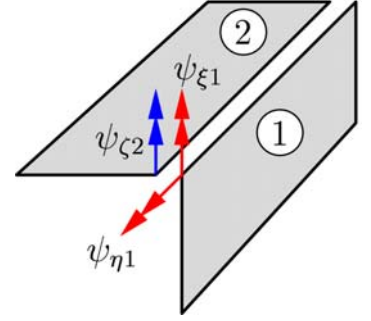


Figure 4: Rotational dof at 2 different elements

Now the SBFEM equation can be written as a matrix differential equation of first order:

$$\begin{pmatrix} \mathbf{u}_{,\xi} \\ \tilde{\mathbf{u}}_{,\xi} \end{pmatrix} = \mathbf{1} \cdot \begin{pmatrix} \mathbf{0} & \mathbf{1} \\ \mathbf{E}_0^{-1} \mathbf{E}_2 & \mathbf{E}_0^{-1} (\mathbf{E}_1 - \mathbf{E}_1^T) \end{pmatrix} \begin{pmatrix} \mathbf{u} \\ \tilde{\mathbf{u}} \end{pmatrix} \quad (22)$$

or simply

$$\boldsymbol{\varphi}_{,\xi} = \mathbf{H} \cdot \boldsymbol{\varphi} \quad (23)$$

The matrix exponential function

$$\boldsymbol{\varphi}(\xi) = e^{\mathbf{H}\xi} \cdot \mathbf{c} = \left(\mathbf{1} + \frac{\mathbf{H}\xi}{1!} + \frac{\mathbf{H}^2 \xi^2}{2!} + \dots \right) \cdot \mathbf{c} \quad (24)$$

solves the differential equation and the vector \mathbf{c} contains the integration constants, which are determined by the boundary conditions.

For positive eigenvalues and $\xi \gg 0$ some entries in $e^{\mathbf{H}\xi}$ become very large which is obvious for an eigenvalue-solution $\boldsymbol{\varphi}_i = e^{\lambda_i \xi} \mathbf{v}_i$ (where $\boldsymbol{\varphi}_i$ is the solution made of the i -th eigenvalue λ_i and the i -th eigenvector \mathbf{v}_i). These solutions are of a significantly larger order of magnitude than the solutions with negative eigenvalues. Due to numerical problems like rounding errors the Jacobian matrix and thus $e^{\lambda_i \xi}$ then become almost singular.

To avoid this problem a shift is introduced. First positive eigenvalues are separated from zero and negative eigenvalues. Like in (Song 2004) a block-diagonal Schur decomposition

$$\mathbf{S} = \mathbf{T}_s^{-1} \mathbf{H} \mathbf{T}_s \quad (25)$$

is used to obtain the block-diagonal Matrix \mathbf{S} .

$$\mathbf{S} = \begin{pmatrix} \mathbf{S}_p & \mathbf{0} & \mathbf{0} \\ \mathbf{0} & \mathbf{S}_0 & \mathbf{0} \\ \mathbf{0} & \mathbf{0} & \mathbf{S}_n \end{pmatrix} \quad (26)$$

Each block is an upper triangular matrix and the elements on the diagonal are the eigenvalues of \mathbf{H} . They are sorted in a way that \mathbf{S}_p contains the positive eigenvalues, \mathbf{S}_0 the zero eigenvalues and \mathbf{S}_n the negative eigenvalues.

Then the matrix exponential with the shift $\xi \rightarrow (\xi - 1)$ is applied, which leads to the solution

$$\boldsymbol{\varphi}(\xi) = \mathbf{T}_s \begin{pmatrix} e^{\mathbf{S}_p(\xi-1)} & \mathbf{0} & \mathbf{0} \\ \mathbf{0} & e^{\mathbf{S}_0 \xi} & \mathbf{0} \\ \mathbf{0} & \mathbf{0} & e^{\mathbf{S}_n \xi} \end{pmatrix} \mathbf{c} = \mathbf{W} \mathbf{c} \quad (27)$$

The integration constants \mathbf{c} are determined by the boundary conditions. For given displacements the corresponding lines of \mathbf{W} (for $\xi=0$ and/or $\xi=1$) are written into a matrix \mathbf{K} . For given loads the lines of $(\mathbf{E}_0 \mathbf{E}_1^T) \mathbf{W}$ are written into \mathbf{K} . And the corresponding displacements and loads are written into a vector \mathbf{f} .

Solving the equation

$$\mathbf{K} \mathbf{c} = \mathbf{f} \quad (28)$$

gives the integration constants \mathbf{c} and the SBFEM equation is solved.

Results

First one single element has been tested. As depicted in figure 5 one end of the element is clamped and at the free end unit-forces and unit-moments are applied. Three different sections are tested. An isotropic section made of steel, a section made of a symmetric

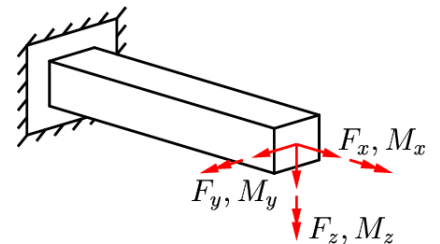


Figure 5: Cantilever beam

laminate $[0,90,\pm 45]_s$ and an asymmetric laminate $[0,90,\pm 45]$. The comparison of the displacements at the free edges with FE simulations gives good results. The element is only a bit too stiff, which is a characteristic of the displacement method used in this work and thus expected.

Then models of thin-walled beams are built up using these new elements. The calculated displacements are compared with those of a FEM-calculation. Three different cross-sections are considered: a plate, an L-profile and a rectangular box. The same three sections as above are tested. The test-case is again the cantilever beam, which is loaded with forces and moments on its free end (see figure 5). The displacements of nodes at the free end are compared with the FEM solution.

In the FE model the thin-walled beam is modeled with rectangular shell elements in ABAQUS. For both FEM and SBFEM the displacements and rotations at the clamped end are suppressed and the load is distributed over the cross-section.

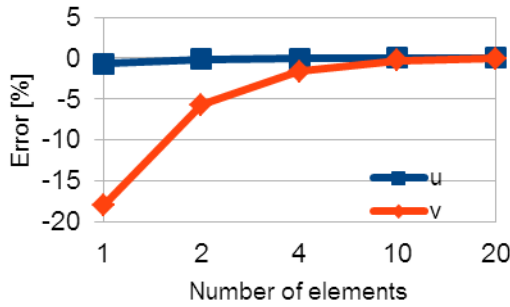


Figure 6: Convergence of SBFEM solution (plate made of asymmetric laminate), u is the displacement into x -direction due to a unit-force in x -direction, v is the displacement into y -direction due to a unit force in y -direction

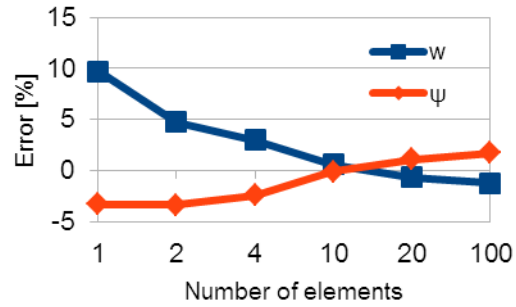


Figure 7: Convergence of SBFEM solution (plate made of asymmetric laminate), w is the displacement into z -direction due to a unit-moment about the x -axis, ψ is the rotation around the x -axis due to a unit moment around the x -axis

In figure 6 and figure 7 the errors of the SBFEM compared to the FEM solution are displayed for the plate with the asymmetric layup. In figure 6 the SBFEM results are seen to converge towards the FEM solution. For the strain of the plate the solution for u is already very good for one element, because the solution doesn't depend on y . For the bending about the z -axis the solution depends on y . Thus the result for v is not very good for one element, but converges rapidly. This rapid convergence is the case for all other loads but the torsion. In figure 7 the convergence for the displacement w of one edge and the rotation angle ψ about the x -axis is shown. The case depicted here is the worst case, but also for the other materials (symmetric laminate or steel) the convergence for torsion is not very good. This may result from missing shear correction factors and is still under investigation.

The results for other cross-sections are quite similar. The results converge quickly as long the elements aren't twisted. When a torsion is applied to a closed cross-section like the rectangular box the elements aren't twisted but only sheared. Thus the convergence is good. But for open cross-sections like a L- or a I-profile the elements are twisted and the convergence gets poor.

Another remarkable result is that the agreement between the FEM and the SBFEM is good for the displacements of leading order. Displacements of a smaller order of magnitude don't match very well. It has to be checked whether this is due to numerical results in the SBFEM or due to a FEM solution which isn't fully converged.

Conclusions and Outlook

In this work a new element for the scaled boundary finite element method has been developed. Its area of application are thin-walled composite beams. Thin-walled sections of a cross-section are modeled with 1 dimensional Timoshenko-like elements which include shear normal to the element. First tests show a quite good convergence.

In further work distributed loads and loads at the side-faces will be included to the method.

An analysis of the strength of the beam is also possible. For that the stresses within each layer have to be calculated, which can be done using the kinematics and the material laws.

Additionally a Hellinger-Reissner functional can be used instead of the Dirichlet functional. Thus shear locking can be avoided and the additional degree of freedom w_m in the middle of the element is no longer required.

Acknowledgement

This work has been performed under the financial support of “Deutsche Forschungsgemeinschaft” under BE 1090/33-1, which is gratefully acknowledged.

References

- Alpdogan, C., Dong, S. and Taciroglu, E. (2010), A method of analysis for end and transitional effects in anisotropic cylinders, *International Journal of Solids and Structures*, 47, pp. 947-956.
- Altenbach, J., Altenbach, H. and Matzdorf, V. (1994a), A generalized Vlasov theory for thin-walled composite beam structures, *Mechanics of Composite Materials*, 30, pp. 43-54.
- Altenbach, J., Kissing, W. and Altenbach, H. (1994b), *Dünnwandige Stab- und Schalenträgerwerke*, Vieweg Verlag Braunschweig
- Argyris, J. and Kačianauskas, R. (1996), Semi-analytical finite elements in the higher-order theory of beams, *Computer Methods in Applied Mechanics and Engineering*, 138, pp. 19-72.
- Artel, J. and Becker, W. (2006), Analysis of free-edge effects by boundary finite element method, *Proceedings in Applied Mathematics and Mechanics*, 6, pp. 205-206.
- Dasgupta, G. (1982), A finite element formulation for unbounded homogeneous continua, *Journal of Applied Mechanics*, 49, pp. 136-140.
- Dieringer, R., Hebel, J. and Becker, W. (2011), The scaled boundary finite element method for plate bending problems, *Proceedings of the 19th International Conference on Computer Methods in Mechanics*, pp. 169-170.
- Dong, S., Kosmatka, J. and Lin, H. (2001), On Saint-Venant's problem for an inhomogeneous anisotropic cylinder: Part I: Methodology for saint-venant solutions, *Journal of Applied Mechanics*, 68, pp. 376-381.
- Gavrić, L. (1994), Finite element computation of dispersion properties of thin-walled waveguides, *Journal of Sound and Vibration*, 173, pp. 113-124.
- Giavotto, V., Borri, M., Mantegazza, P., Ghiringhelli, G., Carmaschi, V., Maffioli, G. and Mussi, F. (1983), Anisotropic beam theory and applications, *Computers & Structures*, 16, pp. 403-413.
- Kosmatka, J., Lin, H. and Dong, S. (2001), On Saint-Venant's problem for an inhomogeneous anisotropic cylinder: Part II: Cross-sectional Properties, *Journal of Applied Mechanics*, 68, pp. 382-391.
- Lin, H., Dong, S. and Kosmatka, J. (2001), On Saint-Venant's problem for an inhomogeneous anisotropic cylinder: Part III: End effects, *Journal of Applied Mechanics*, 68, pp. 392-398.
- Mayland, W. and Becker, W. (2010), Investigation of Stress Singularities due to Geometrical and Material Discontinuities in Piezoelectric Laminates by the Scaled Boundary Finite Element Method, *International Journal of Advances in Mechanics and Applications of Industrial Materials*, 1, pp. 11-17.
- Morandini, M., Chierichetti, M. and Mantegazza, P. (2010), Characteristic behavior of prismatic anisotropic beam via generalized eigenvectors, *International Journal of Solids and Structures*, 47, pp. 1327-1337.
- Reddy, J.N. (1997), On locking-free shear deformable beam finite elements, *Computer Methods in Mechanics and Engineering*, 149, pp. 113-132.
- Schardt, R. (1989), *Verallgemeinerte technische Biegetheorie*, Springer Verlag Berlin.
- Silvestre, N. and Camotim, D. (2002), First-order generalized beam theory for arbitrary orthotropic materials, *Thin-Walled Structures*, 40, pp. 755-789.
- Song, C. (2004), A matrix function solution for the scaled boundary finite-element equations in statics, *Computer Methods in Applied Mechanics and Engineering*, 193, pp. 2325-2356.
- Taweel, H., Dong, S. and Kazic, M. (2000), Wave reflection from the end of a cylinder with an arbitrary cross-section, *International Journal of Solids and Structures*, 37, pp. 1701-1726.
- Tisseur, F. and Meerbergen, K. (2001), The Quadratic Eigenvalue Problem, *SIAM Review*, 43(2), pp.235-286.
- Wolf, J. P. and Song, C (1996), *Finite-element modelling of unbounded media*, Wiley Chichester, England.
- Wolf, J. P. (2002), *The Scaled Boundary Finite Element Method*, Wiley Chichester, England
- Yang, P., Norris, C. and Stavsky, Y. (1966), Elastic wave propagation in heterogeneous plates, *International Journal of Solids and Structures*, 2, pp. 665-684.